

Fig. 1. A schematic diagram of a conventional Shack-Hartmann wavefront sensor, and a typical spot pattern with 64 sub-apertures (4096 detector pixels).

Shack-Hartmann sensor improvement using optical binning

Alastair Basden, Deli Geng, Dani Guzman, Tim Morris, Richard Myers, Chris Saunter

Department of Physics, South Road, Durham, DH1 3LE, UK

We present a design improvement for a recently proposed type of Shack-Hartmann wavefront sensor that uses a cylindrical (lenticular) lenslet array. The improved sensor design uses optical binning and requires significantly fewer detector pixels than the corresponding conventional or cylindrical Shack-Hartmann sensor, and so detector readout noise causes less signal degradation. Additionally, detector readout time is significantly reduced, which reduces the latency for closed loop systems, and data processing requirements. We provide simple analytical noise considerations and Monte-Carlo simulations, and show that the optically binned Shack-Hartmann sensor can offer better performance than the conventional counterpart in most practical situations, and our design is particularly suited for use with astronomical adaptive optics systems. © 2018 Optical Society of America

OCIS codes: 010.1080, 010.7350

1. Introduction

A conventional Shack-Hartmann sensor (SHS) divides a pupil into sub-apertures using a lenslet array and attempts to measure the wavefront gradients in orthogonal directions across each sub-aperture as shown in Fig. 1. Estimation of the wavefront gradients typically involves finding the centre-of-mass of the image spot created in the sub-aperture (the mean light position). This is typically done by software binning of the measured light signal in one direction when computing the algorithm, and then computing the dot product of this vector with an index vector (i.e. a vector counting from 0 to $N-1$ where N is the number of pixels in a sub-aperture). Computation of the corresponding orthogonal wavefront tilt is carried out by software binning the measured light signal in the orthogonal direction. Once these spot centroid locations have been retrieved, a reconstruction algorithm is used to provide an estimate of the wavefront under investigation.

Here, we present a modified version of the SHS described by Ares et al. [1]. This design uses the cylindrical lenslet array proposed previous, and also implements optical signal binning. There are a number of situations where this can give a performance improvement when compared with a conventional SHS which we describe in §2. The original cylindrical Shack-Hartmann sensor design described by Ares [1] was intended to provide a reliable way to measure wavefront gradients outside the nominal Shack-Hartmann lenslet area on the detector, such as when there are highly aberrated wavefronts or abrupt phase changes, for time-static aberrations. The design proposed here has an additional aim, to achieve higher wavefront sensor (WFS) frame-rates than would be possible using a conventional SHS, by using fewer detector pixels, and also to give improved signal to noise ratio (SNR) performance.

A simplified schematic of an Optically binned SHS (OBSHS) is given in Fig. 2, along with an example for the detector images. The wavefront is first split with a 50/50 beam-splitter. Each of the resulting beams then passes through one of two identical cylindrical (lenticular) lenslet arrays oriented orthogonally, some cylindrical re-imaging optics (not shown here for clarity, see Fig. 3), and onto separate detectors. A conventional (circular) lenslet array focuses the wavefront in two directions, giving a conventional point-spread function. Conversely, the cylindrical lenslet arrays proposed here focus the wavefront in only one direction. Rather than a single spot, light will be spread along a number of lines as shown in Fig. 2.

The two orthogonal lenslet arrays are required to measure orthogonal wavefront gradients. The design described by Ares [1] used a single cylindrical array which was rotated by 90° to measure the orthogonal wavefront gradients, rather than the beam splitter shown here. A drawback of this technique is that it is only suitable for characterising static aberrations, as detector images have to be captured before and after the precise 90° rotation.

In order to minimise the number of detector pixels required for wavefront gradient estimation, the OBSHS should be designed such that the width of the focused line (Fig. 2(b) and (c)) is n_s detector pixels wide where n_s is the number of sub-apertures in each dimension (i.e. there are $n_s \times n_s$ sub-apertures in total). This means that a one-dimensional centre-of-mass calculation for the line position in the direction orthogonal to the line will give the corresponding centroid location and wavefront gradient estimate in this direction for this sub-aperture, i.e. by measuring the offset of the line from the nominal origin position of each sub-aperture. Each sub-aperture is one pixel wide and a larger number (n_l , e.g. eight) pixels long, depending on the field of view required. When the advanced processing techniques for line location are used [1], the number of pixels orthogonal to the cylindrical lenslet direction (n_l) can be reduced compared with a conventional SHS, whilst achieving the same field of view. These processing techniques effectively apply a continuity condition to the measured line position, and greatly reduce the problem of sub-aperture cross-talk, except for when the local wavefront tilt is great enough to place light from one sub-aperture on top of another.

Unless the detector has elongated pixels, it will be necessary to use non-symmetrical re-imaging optics to compress the image in one dimension, such that each sub-aperture is then one pixel wide and n_l pixels long (so that the wavefront gradient can be detected in this direction). These re-imaging optics can consist of two cylindrical lenses as shown in Fig. 3(b).

A similar idea has previously been used for the NAOMI instrument of the William Herschel Telescope (WHT) [2], and the SWAT adaptive optics (AO) system [3], using a conventional lenslet array and electronic binning in the detector (before readout), rather than optical binning. This will achieve a similar effect though will suffer from higher dark current and a lower readout rate than the OBSHS described here.

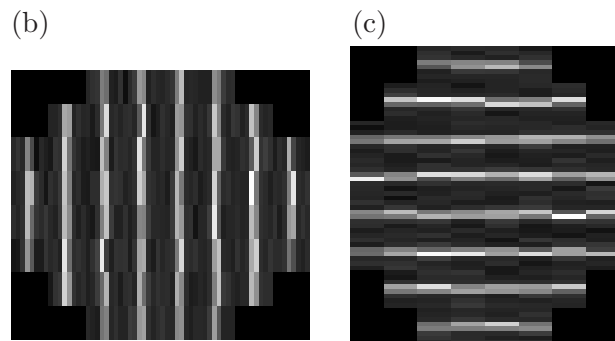
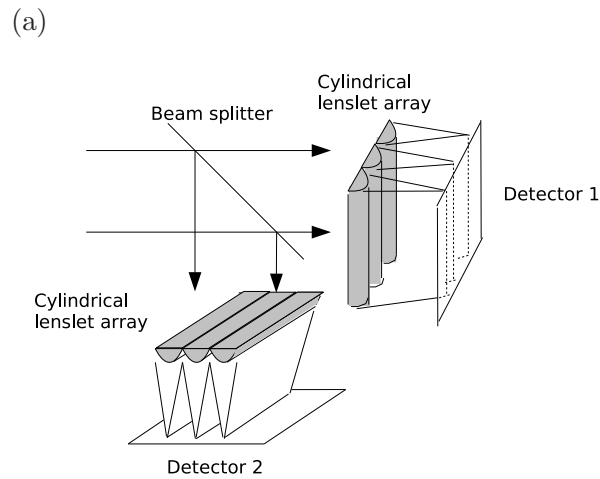


Fig. 2. (a) A schematic diagram of an optically binned Shack-Hartmann wavefront sensor. The incoming wavefront is split using a beam splitter, and each beam then passes through orthogonal cylindrical lenslet arrays, to record the x and y wavefront gradients on separate detectors. (b) A typical resulting image from detector 1 (512 detector pixels, 8×8 sub-apertures, vertical lenslet array). (c) A typical resulting image from detector 2 (512 detector pixels, 8×8 sub-apertures, horizontal lenslet array). Elongated rectangular detector pixels have been used in (b) and (c) to make the image clearer.

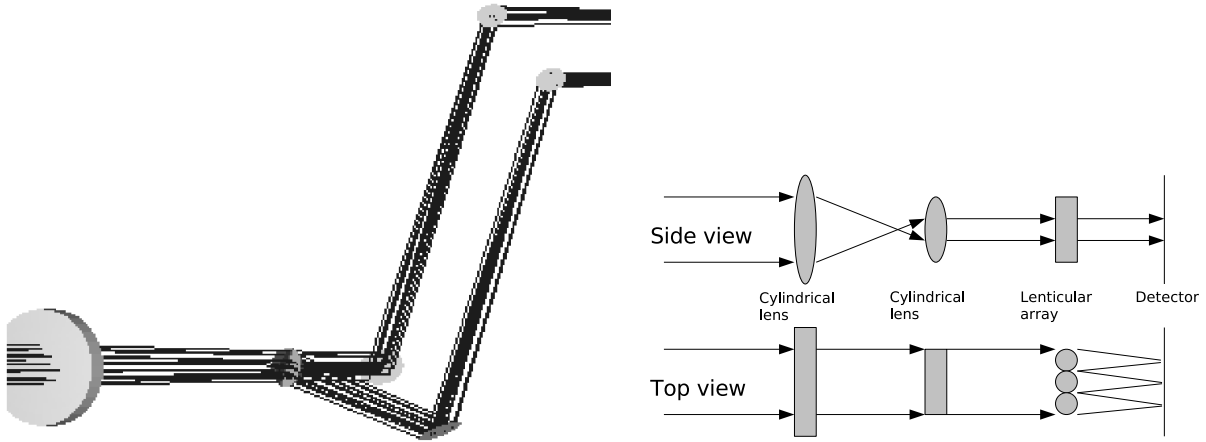


Fig. 3. A schematic diagram showing possible sub-designs for an optically binned Shack-Hartmann sensor, (a) using fold mirrors to rotate the reflected beam by 90° (b) using shared cylindrical optics for each beam, one beam shown, to compress the phase in one dimension relative to the other.

2. Practical design of an optically binned Shack-Hartmann sensor

When designing an OBSHS, the impact of mis-alignment between the two orthogonal sensor directions needs to be considered. To overcome this effect, a 90° beam rotation can be introduced to the reflected arm of the sensor, using two fold mirrors, the first of which directs light out of the beam splitter plane, and the second then directs light so that it is going in the same direction as the beam transmitted through the beam splitter. Two fold mirrors can also be used with transmitted beam so that both beams are then at the same height (see Fig. 3(a)), and if these fold by more than 90° back on themselves, the path length of the two beams can be equalised. Accurate alignment of these beams should be possible using standard techniques for mirror alignment. Both beams can then be passed through the same cylindrical lenses and lenslet array, and detected using the same detector, which greatly simplifies the system, and improves stability. By using the same lenses and lenslet array for each beam, we can ensure that truly orthogonal wavefront gradients are measured. Fig. 3 shows a possible design for the OBSHS. This design requires two cylindrical lenses to image the line pattern onto the detector, compressed in one dimension.

It is also possible to use a conventional lenslet array rather than a cylindrical (lenticular) array, if this is more readily available, though this will require more additional optics. In this case, after the lenslet array, one conventional lens (to collimate the sub-apertures), the beam splitter, two cylindrical lenses (to compress in one dimension) and then a conventional lens (to image onto the detector) are required for each beam. The cylindrical lenses are used to compress the image in one dimension, so that the sub-aperture images in this dimension are only one pixel wide.

If a locally generated shuttered plane wave is included, injected at the beam splitter, this can be used as a sub-aperture tilt reference during calibration of the system, as proposed by [4]. By adding a calibrated tilt mirror to the reference path, both the orthogonality and absolute magnitude of the sub-aperture tilts can be calibrated. This allows fine tuning of the optical train, and also provides an empirical basis set for reconstruction matrix generation, matched to the actual hardware.

2.A. Advantages of optical binning

There are several advantages for an OBSHS related to the reduced number of detector pixels required, in addition to those previously mentioned [1]. For example, if a conventional SHS uses 8×8 pixels per sub-aperture, the equivalent optically binned sensor will require eight pixels per sub-aperture for two orthogonal directions (16 pixels in total), or fewer if advanced line detection algorithms are used. This means that smaller detector arrays can be used, and frame rate can be correspondingly higher, reducing latency due to readout time in closed loop systems, which will improve the performance of these systems. Additionally, the use of fewer pixels means that detector read-noise is reduced and so the SNR can be increased. Computational and data bandwidth requirements are also reduced, an important consideration for next generation astronomical AO systems.

Systems that may have performance improved by using an OBSHS will have $n_l > 2$. This will include any open-loop WFS system, such as deformable mirror (DM) figure sensor detectors for multi-object adaptive optics (MOAO) applications: Open-loop control of deformable mirror elements by the AO loop means that precise knowledge of their figure at any given time is necessary, and can be obtained using a figure sensor. In §3.E, we discuss the requirements for one particular figure sensor.

2.B. Disadvantages of optical binning

The light used in each orthogonal centroid calculation is halved by the beam splitter. In most situations this disadvantage is overcome by the reduction in detector readout noise due to the use of fewer detector pixels. However, for closed loop systems, this may not be the case. For such systems (once the loop has been closed), the wavefront can be assumed to be nearly flat within each sub-aperture, and so the Shack-Hartmann spot is close to the null position, and a small number of pixels (typically 2×2) can be used to estimate the centroid location. Signal and noise is therefore obtained from four pixels. In the optically binned case, half the light is used to estimate the centroid location for each orthogonal direction, and likewise half the pixels are used (two) for each direction resulting in a lower SNR than in the conventional case. It should be noted that this is an extreme case, and most Shack-Hartmann sensors will use more pixels per sub-aperture even when the loop is closed, giving an advantage to the optically binned sensor. The OBSHS also uses extra optics compared with a conventional SHS, two fold mirrors, and possibly the two cylindrical lenses (most conventional systems will contain the same number of lenses for re-imaging and scaling purposes). This therefore results in a slightly reduced throughput, though reflectivity of these mirrors can be very high.

3. Optically binned SHS performance

We compare the performance of an OBSHS with a conventional SHS using simple analytical considerations, and Monte-Carlo simulation of a closed loop astronomical AO system, the results of which are described here.

3.A. Analytical performance estimates

In general, the signal s for the conventional SHS will be offset by the detector readout noise and photon shot noise scaling as $\sqrt{s + (N^2\sigma)^2}$, N being the number of pixels in one dimension of each sub-aperture and σ being the detector readout noise for a single pixel, giving a SNR of $\frac{s}{\sqrt{s + (N^2\sigma)^2}}$.

For the OBSHS, the signal will be $\frac{s}{2}$, and the noise will scale as $\sqrt{\frac{s}{2} + (N\sigma)^2}$, giving a SNR of $\frac{\frac{s}{2}}{\sqrt{\frac{s}{2} + (N\sigma)^2}}$. The optically binned case therefore gives better performance for $N > 2$ when detector

readout noise is greater than about five electrons, for all light levels. When detector readout noise is one electron, the OBSHS gives better performance for $N > 5$ for all light levels, or $N > 2$ when $s < 40$ photons. For a noiseless detector, the OBSHS always gives worse SNR performance (by a factor of $\frac{1}{\sqrt{2}}$). For a low noise detector with $\sigma = 0.1$ electrons (e.g. an electron multiplying CCD (EMCCD)), the OBSHS gives better SNR performance when $N > 6$ for $s > 20$, which will be the case in most practical situations.

It should be noted that two-dimensional weighted centroid calculations [5] which raise the detector signal from each pixel by a given power (typically 1.5) before spot centroid location determination, cannot be used with the OBSHS since binning of the signal has already occurred. However, a similar one-dimensional weighting algorithm can be used.

3.B. Closed loop adaptive optics Monte-Carlo simulation comparisons

The performance of an OBSHS and a conventional SHS have been compared using the Durham AO simulation platform [6]. This software simulation comprises a classical AO system on a 42 m telescope for each WFS (one DM, one natural guide star (NGS), also the science target), and light for each WFS passes through the same atmospheric turbulence, as shown in Fig. 4. The atmospheric turbulence was simulated using the frozen turbulence model [7], with a ground layer, and layers at 200 m and 2 km (all uncorrelated, moving in different directions at different speeds). Except when otherwise stated, the wavefront sensor was assumed to have three electrons read-noise, using a 13th magnitude guide star (5 ms integration time), 32×32 sub-apertures with 8 pixels per sub-aperture. The effect of feedback-loop latency was not investigated, though since this will be reduced for the OBSHS (fewer pixels), the true performance of the OBSHS is likely to be further improved relative to a conventional SHS in closed loop situations. Further results of the simulation are not given here as they would add length but not value to this paper, as only the relative performance of the two WFSs are of interest here.

3.C. Simulation results

The effect on performance of several critical AO system parameters has been investigated, and the Strehl ratio of an image obtained using the AO corrected wavefront is used as a performance estimator (a perfectly flat wavefront will give a Strehl ratio of unity). The effect of guide star magnitude on the relative performance of the conventional SHS and the OBSHS was investigated, and results shown in Fig. 5. It can be seen that the OBSHS offers better relative performance as the source grows fainter (at the lowest light level, the loop was not able to close in either case). This is predicted by the simple SNR calculations.

The effect of detector readout noise was also investigated, and Fig. 6 shows that for detectors with a non-zero readout noise, the OBSHS performance is better, due to there being fewer detector pixels required.

The effect on performance of the number of sub-apertures used is shown in Fig. 7, and shows that the OBSHS gives better performance than the conventional SHS. Higher order correction is given as the number of sub-apertures increases. However, light is then shared between more sub-apertures, and so image correction eventually becomes worse.

Similarly, as the number of pixels per sub-aperture is varied, the OBSHS gives better performance relative to the conventional SHS, as shown in Fig. 8. As the number of pixels increases, light is shared between more pixels, meaning that readout noise has a more dominant effect, resulting in poorer correction. When too few pixels are used, correction is also poor, as the AO loop is difficult to close.

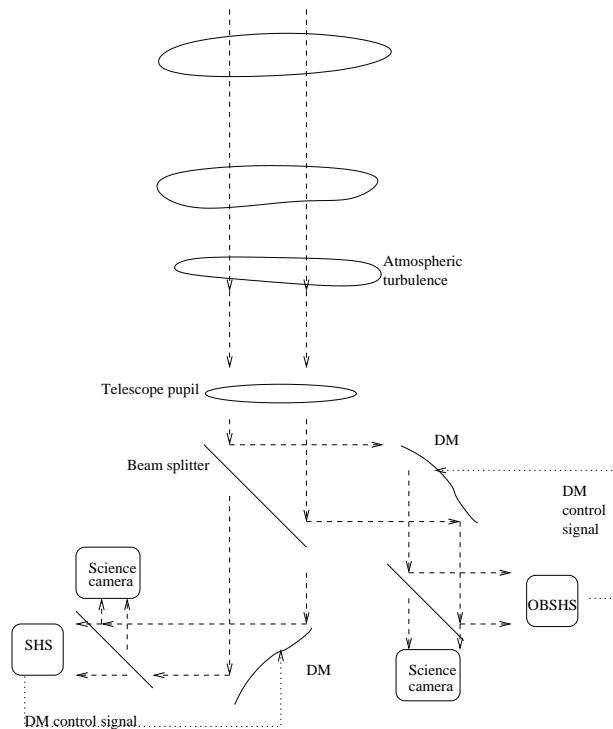


Fig. 4. A schematic diagram of the components of a Monte-Carlo simulation used to compare wavefront sensor performance. A simulated beam-splitter is used to direct half the light to a conventional AO and imaging system, while the other half is directed to an optically binned AO system. The performance of these systems can then be directly compared.

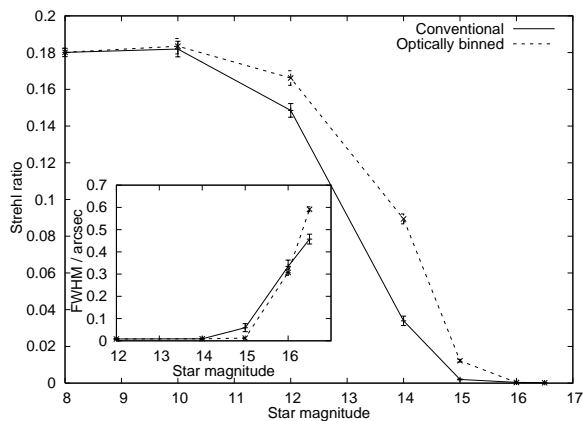


Fig. 5. A figure showing the relative performance between a conventional and optically binned SHS as a function of source magnitude. The inset shows the FWHM as a function of magnitude.

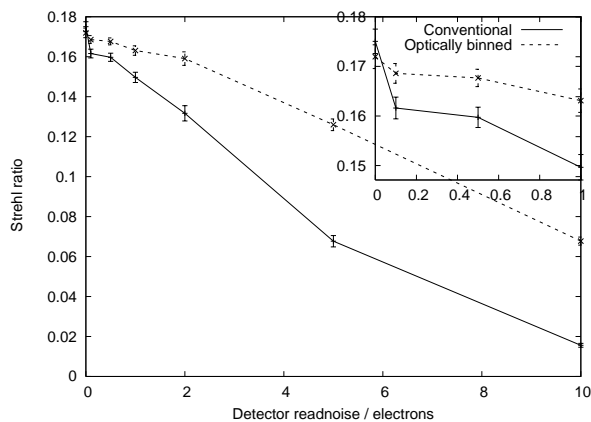


Fig. 6. A figure showing the relative performance between a conventional and optically binned SHS as a function of detector readout noise. Inset is the results for 0–1 electron readout noise in more detail.

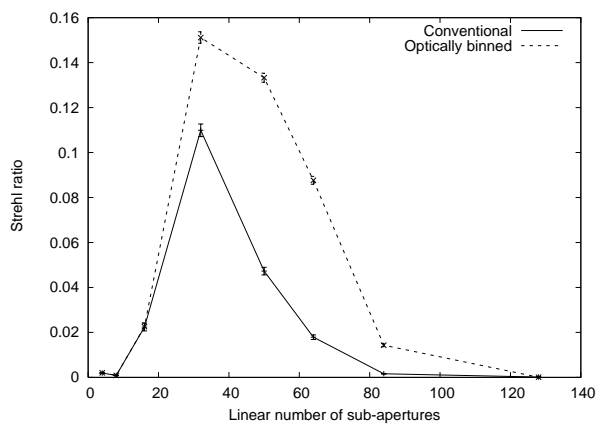


Fig. 7. A figure showing the relative performance between a conventional and optically binned SHS as a function of the linear number of sub-apertures.

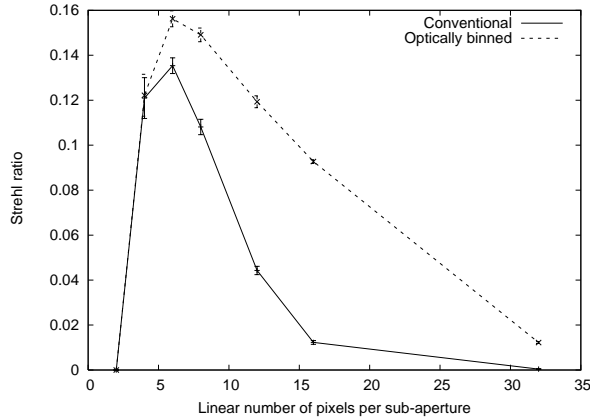


Fig. 8. A figure showing the dependence on relative performance between a conventional and optically binned SHS with the number of pixels per sub-aperture (linear dimension, so for the conventional case, the total number is this squared, while for the optically binned case, the total number is this multiplied by two).

3.D. Simulation conclusions

The extensive, but not exhaustive parameter space search carried out to compare the performance of a conventional SHS and OBSHS shows that the OBSHS can give better closed loop AO performance in most situations, in agreement with a simple consideration of signal and noise sources in the WFSs.

3.E. Case study: DUGALL figure sensor

The Durham University generalised adaptive optics laser laboratory (DUGALL) is a proposed high-order on and off-sky laser guide star (LGS) test facility. It will have several operational modes, including MOAO and laser tomographic adaptive optics (LTAO). MOAO involves open loop wavefront sensing and mirror shaping (the WFS does not view the DM), and relies on the shape of the unsensed deformable mirror being known at all times. Typically this could involve strain gauges [8] or direct measurement of the mirror shape, since hysteresis and non-linearities within the mirror will mean that the shape of the mirror is not always equal to the initially requested shape. DUGALL proposes to use a 4 K actuator Micro-Electro-Mechanical Systems (MEMS) deformable mirror, which does not contain strain gauges, and so direct measurement of the mirror shape is required using a figure sensor. Figure sensing must ideally operate at several times the rate of the AO loop, so that several adjustments to the mirror shape can be made during each AO loop iteration, until the desired shape is reached. The DUGALL AO loop will have a maximum operational rate of 1 kHz, and so the figure sensor may require a frame rate of up to 10 kHz, depending on the accuracy (time-resolution) required and control algorithms used. Since the figure sensor measures the shape of a non-null (non-flat) mirror, wavefront gradients can be significant, and so a reasonable field of view is required for each sub-aperture, giving rise to a requirement of 8×8 pixels for a conventional SHS. The 4 K deformable mirror has 64×64 actuators, and so a SHS of this order is required. If a conventional SHS sensor is used, this would require a detector capable of reading a 512×512 array at 10 kHz, and a platform for computing centroid locations in real-time, requiring a data rate of 5 GBs^{-1} , assuming two bytes per pixel. We are unaware of a suitable commercially available sensor able to meet these requirements.

By using an OBSHS, we would require two sensors each with 64×512 pixels, and a reduced data rate of about 500 MBs^{-1} for each sensor. There are several readily available commercial sensors that would meet this requirement. The reduced data rate makes centroid computation less demanding in real-time, and the OBSHS will also give an improvement in SNR. We are currently developing such a WFS.

4. Conclusions

We have presented an improved design for a Shack-Hartmann WFS, using optical binning and a cylindrical lenslet array. This design promises to improve the SNR for wavefront reconstruction in most situations, and involves splitting the wavefront for detection of the orthogonal wavefront gradients, using an optically binned SHS. We have presented general Monte-Carlo simulation results which show that this OBSHS can lead to better performance than a conventional SHS, and have presented schematic designs for such a detector. This WFS will be of particular interest for open loop systems where the wavefront gradients can be large, requiring many pixels per sub-aperture for detection, and for systems where a high frame-rate and low latency is important.

References

1. M. Ares, S. Royo, and J. Caum, “Shack-Hartmann sensor based on a cylindrical microlens array,” *Optics Letters* **32**, 769–771 (2007).
2. R. M. Myers, A. J. Longmore, C. R. Benn, D. F. Buscher, P. Clark, N. A. Dipper, N. Doble, A. P. Doel, C. N. Dunlop, X. Gao, T. Gregory, R. A. Humphreys, D. J. Ives, R. Øestensen, P. T. Peacocke, R. G. Rutten, C. J. Tierney, A. J. A. Vick, M. R. Wells, R. W. Wilson, S. P. Worswick, and A. Zadrozny, “NAOMI adaptive optics system for the 4.2m William Herschel telescope,” in “Adaptive Optical System Technologies II. Edited by Wizinowich, Peter L.; Bonaccini, Domenico. Proceedings of the SPIE, Volume 4839, pp. 647-658 (2003).”, , vol. 4839 of *Presented at the Society of Photo-Optical Instrumentation Engineers (SPIE) Conference*, P. L. Wizinowich and D. Bonaccini, eds. (2003), vol. 4839 of *Presented at the Society of Photo-Optical Instrumentation Engineers (SPIE) Conference*, pp. 647–658.
3. H. T. Barclay, P. H. Malyak, W. H. McGonagle, R. K. Reich, G. S. Rowe, and J. C. Twichell, “The SWAT wavefront sensor,” *Lincoln Laboratory Journal* **5**, 115–130 (1992).
4. L. E. Schmutz, B. J. K., F. J., and T. S., “Integrated Imaging Irradiance (I3) sensor: a new method for real-time wavefront mensuration,” in “Adaptive Optical Components II. Edited by Holly, Sandor ; James, Lawrence. Proceedings of SPIE, Volume 141, pp. 120-124,” , vol. 141 of *Presented at the Society of Photo-Optical Instrumentation Engineers (SPIE) Conference*, S. Holly and L. James, eds. (1979), vol. 141 of *Presented at the Society of Photo-Optical Instrumentation Engineers (SPIE) Conference*, pp. 120–124.
5. S. Thomas, T. Fusco, A. Tokovinin, M. Nicolle, V. Michau, and G. Rousset, “Comparison of centroid computation algorithms in a Shack-Hartmann sensor,” *MNRAS* **371**, 323–336 (2006).
6. A. G. Basden, T. Butterley, R. M. Myers, and R. W. Wilson, “Durham extremely large telescope adaptive optics simulation platform,” *Applied Optics* **46**, 1089–1098 (2007).
7. G. I. Taylor, “The spectrum of turbulence,” *Proc. R. Soc. London, Ser. A* **164**, 476–490 (1938).
8. C. R. Benn, M. Blanken, C. Bevil, S. Els, S. Goodsell, T. Gregory, P. Jolley, A. J. Longmore, O. Martin, R. M. Myers, R. Ostensen, S. Rees, R. G. M. Rutten, I. Soechting, G. Talbot, and S. M. Tulloch, “NAOMI: adaptive optics at the WHT,” in “Advancements in Adaptive Optics. Edited by Domenico B. Calia, Brent L. Ellerbroek, and Roberto Ragazzoni. Proceedings of the SPIE, Volume 5490, pp. 79-89 (2004).”, , vol. 5490 of *Presented at the Society of Photo-Optical Instrumentation Engineers (SPIE) Conference*, D. Bonaccini Calia, B. L. Eller-

broek, and R. Ragazzoni, eds. (2004), vol. 5490 of *Presented at the Society of Photo-Optical Instrumentation Engineers (SPIE) Conference*, pp. 79–89.